

PHASE RELATIONS OF AgVO_3 FORMED FROM VANADIUM PENTOXIDE HYDRATE SOL IN RELATION WITH THE ELECTRIC CONDUCTIVITY

Shigeharu Kittaka, Miyuki Kawata, Naoko Wada, Satoshi Ono, and Haruo Akashi*

Department of Chemistry, Faculty of Science, Okayama University of Science, 1-1 Ridaicho, Kita-ku, Okayama 700-0005, Japan e-mail: kittaka@chem.ous.ac.jp

*Research Institute of Natural Sciences, Okayama University of Science, 1-1 Ridaicho, Kita-ku, Okayama 700-0005, Japan

(Received August 28, 2015; accepted November 9, 2015)

Key words: AgVO_3 ; Phase properties; Ionic conductivity,

The interrelation of AgVO_3 polymorphs was studied using X-ray diffraction (XRD), neutron diffraction (ND), differential scanning calorimetry, and electrical conductivity measurements. α - AgVO_3 and δ - AgVO_3 were shown to be metastable phases while β - AgVO_3 is a stable phase. The α - AgVO_3 is reversibly transformed into a deformed form of α - AgVO_3 at around 160 °C and irreversibly to β - AgVO_3 at 250 °C. Electrical conduction for β - AgVO_3 and δ - AgVO_3 increase with temperature (100-400 °C), which has been ascertained using XRD measurements. The amorphous phase crystallized into β - AgVO_3 through α - AgVO_3 . From these facts, phase relations are proposed for amorphous AgVO_3 , α - AgVO_3 , δ - AgVO_3 , β - AgVO_3 , and deformed forms of the latter three samples. The electrical conductivity of the higher-temperature phase of the three samples demonstrates that they are superionic conductors with conductivities above $10^{-3} \text{ S cm}^{-1}$. The crystal parameters of δ - AgVO_3 were determined using high-resolution XRD diffraction with BL02B1 beamline in SPring-8 (Super Photon ring-8 GeV) and powder neutron scattering using Vega at KEK (Koh Energy Kasokukikikoh: laboratory for high energy acceleration system).

∴

Introduction

Metal vanadate compounds have many variations with various metal ions and oxidation states, and can be conventionally formed by heating a mixture of component metal, metal oxides, and/or thermally decomposable metal salts with V_2O_5 . The authors have recently formed three AgVO_3 phases (α -, β -, and δ -types) from aqueous systems by reacting vanadium pentoxide hydrate ($\text{V}_2\text{O}_5 \cdot n\text{H}_2\text{O}$) sol with AgNO_3 solution.¹⁾ β - AgVO_3 was found to be a stable phase while α - AgVO_3 was a metastable phase.²⁾ The crystal structure of the newly found δ - AgVO_3 has not yet been determined.

There are several ionic conductors including silver ions in both crystalline and/or glassy states. Silver

vanadates have so far been used to prepare a glassy state of the solid, a mixed molten phase with Ag_2O and V_2O_5 .^{3,4)} The main reason for this is that the silver vanadates can be molten at rather low temperatures of around 500 °C. To our knowledge, however, there are no reports concerning electrical conductivity measurements of AgVO_3 shown above.

The present paper reports electrical conductivity measurements on α - AgVO_3 , β - AgVO_3 , and δ - AgVO_3 in relation to their crystal structures. Electrical conductivity measurements of these samples led us to find new reversible phase changes at a temperature below the irreversible transition from α - AgVO_3 to β - AgVO_3 , and below the melting points of β - AgVO_3 and δ - AgVO_3 .

The crystal structure of δ -AgVO₃ was analyzed using single-crystal X-ray diffraction (XRD) and neutron diffraction (ND) of the powder form, but not definitively. Some comments on the result are given in the last section.

Experimental

Materials. A reaction diagram was prepared by varying the ratio of vanadium pentoxide hydrate, V₂O₅·*n*H₂O, and AgNO₃ solutions, in which some additional ratios were tested to those used in the previous work.¹⁾ All of the precipitates were obtained as needle-like fine particles, a few micrometers in length.

Electrical conductivity measurements. Electrical conductivity was determined by measuring the DC conductivity. The measured specimens were prepared as follows. α -AgVO₃ and β -AgVO₃ blocks were prepared by cooling the melt of α -AgVO₃ (550 °C) quickly in ice water and slowly (7 °C h⁻¹), respectively. The sample block was shaped to size (diameter 5 mm and length 7 mm), on both ends of which Ag paste was placed to form electrodes for the electric circuit.⁵⁾ With this electrode system, the measured conductivity is composed of both electronic (or electron hole) and ionic (Ag⁺) contributions. The dried δ -AgVO₃ precipitate was pressed into a disk (2 mm thickness and 1 cm diameter) and calcined in advance at 420 °C for 5 h in air. Samples were set in a glass chamber and contacted with 1 atm O₂ after evacuation. The measuring setup was composed of a DC power supply (544B, Metronix Co.), electrometer (AM-1001, Ohkura Elec. Co.), and a microampere meter (Yokogawa Electric Works).

Crystal structures. The temperature effect on the powder XRD measurements was determined using a sample holder designed for high-temperature measurements in air. The apparatus used was a Rigaku RAD-2R, which was equipped with a Cu target X-ray tube and home-made sample holder. A single crystalline form of δ -AgVO₃ (3 × 8 × 135 μm³) was analyzed at BL02B1 beam line in SPring-8 (λ = 0.33100 Å). Neutron-diffraction measurements using Vega at KEK were also conducted for the powder form of δ -AgVO₃, which was repeatedly preheated at 300 °C and ground for better crystallinity and better homogeneity of crystallite size distribution. The prepared sample was used also for analysis of the diffraction pattern measured with RAD-2R.

Thermodynamic measurements. Thermal properties of the samples were studied using differential thermal analysis (DTA) (25–600 °C) and/or differential scanning calorimetry (DSC) (<400 °C). The enthalpy change of the phase change was determined by calibrating with the enthalpy of melting of pure In. ULVAC TGD-7000 and DSC-7000 were used for these measurements.

Results and Discussion

1. Reaction phase diagram. Figure 1 shows the reaction phase diagram prepared from V₂O₅·*n*H₂O sol and AgNO₃ solutions, in which both axes indicate the concentration of each component in the system.

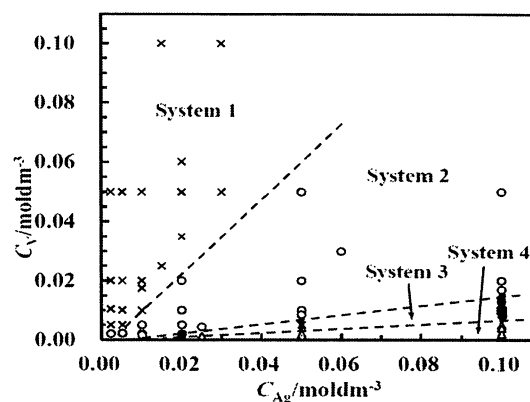


Fig. 1. Formation phase diagram of the V₂O₅·*n*H₂O–AgNO₃ aqueous systems at room temperature, presenting the characteristic sediments or crystalline particles.

The diagram can be divided into four areas dependent upon the structure of the sediments: System-1, an intercalation compound of V₂O₅·*n*H₂O (Ag_{0.33}V₂O₅·*n*H₂O); System-2, α -AgVO₃ and hydrous phase of Ag_{2-x}V₄O₁₁; System-3, δ -AgVO₃; System-4, β -AgVO₃.

Phase changes for System-1 through System-3 are easily achieved by increasing Ag⁺ content.⁴⁾ However, System-3 was not forced by Ag⁺ addition to move into the System-4 or other form, even though a fairly large amount was introduced. Thus, δ -AgVO₃ is, once formed, quite resistant. Apparently, it is not possible to define which phase is the most stable phase between β -AgVO₃ and δ -AgVO₃ under ambient conditions.

The stability of the phase can be assessed using the Gibbs free energy relation [1]:

$$d\Delta G = -\Delta SdT + \Delta VdP, \quad [1]$$

where ΔG and ΔV are the free energy and molar volume differences between the two phases; in equilibrium, the former is zero. ΔS is the entropy difference and should be equal to the heat of transition divided by the temperature. Pycnometry of both substances gave the densities 5.39 g cm^{-3} for $\beta\text{-AgVO}_3$ and 5.01 g cm^{-3} for $\delta\text{-AgVO}_3$, i.e., $\Delta V < 0$. Thus, higher pressure is needed to transform $\delta\text{-AgVO}_3$ into $\beta\text{-AgVO}_3$. Because both phases are molten at the same temperature of $474 \text{ }^\circ\text{C}$, we can determine the enthalpy difference from the heats of melting¹ and assign the larger molar enthalpy to $\delta\text{-AgVO}_3$ than to $\beta\text{-AgVO}_3$ by 0.9 kJ mol^{-1} . This suggests that a temperature decrease is required if the transformation of $\delta\text{-AgVO}_3$ to $\beta\text{-AgVO}_3$ is required. These contributions were investigated using the hydrothermal treatment of $\delta\text{-AgVO}_3$.

Figure 2 shows the effect of hydrothermal heat treatment on the structure of $\delta\text{-AgVO}_3$. Treatment of $\delta\text{-AgVO}_3$ at $200 \text{ }^\circ\text{C}$ under a hydrothermal pressure of 15 atm (b and c) brings about the deformation and recrystallization into (e) $\beta\text{-AgVO}_3$. Hydrothermal treatment at $80 \text{ }^\circ\text{C}$ for the long period of 15 months

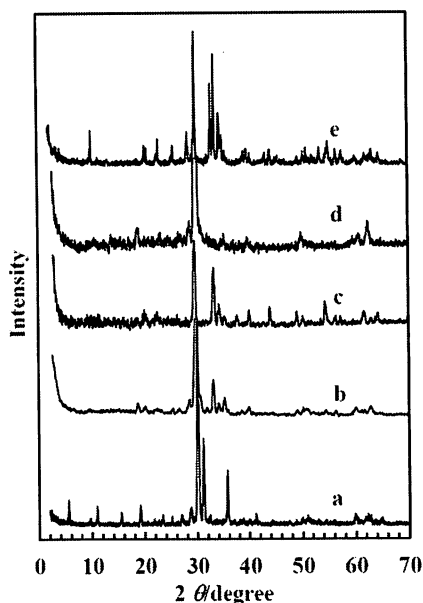


Fig. 2. Changes in XRD patterns of $\delta\text{-AgVO}_3$ to $\beta\text{-AgVO}_3$ using hydrothermal treatments. (a) $\delta\text{-AgVO}_3$; treatment conditions (b) 15 atm, $200 \text{ }^\circ\text{C}$, 24 h; (c) 15 atm, $200 \text{ }^\circ\text{C}$, 10 days; (d) 1 atm at $80 \text{ }^\circ\text{C}$; (e) $\beta\text{-AgVO}_3$.

produced decomposition of crystalline $\delta\text{-AgVO}_3$. It is not possible to identify the structure of the product with any other form of AgVO_3 . This fact is the oppo-

site direction to the thermodynamic measurement. These results do not coincide either with the fact that heat treatment in air did not affect the crystal structure up to the melting point.¹⁾ Thus, we may say that $\delta\text{-AgVO}_3$ is a metastable phase, and cannot be transformed into other phases under dry conditions. Furthermore, the presence of water is important for the transition to give a stable phase, e.g., the dissolution and precipitation processes act to grow $\beta\text{-AgVO}_3$. Hydrothermal treatment in an autoclave at $200 \text{ }^\circ\text{C}$ under about 15 atm accelerated the change of $\delta\text{-AgVO}_3$ to $\beta\text{-AgVO}_3$, which is favorably accompanied by the volume change.

2. *Electrical conductivity of AgVO_3 .* Figure 3 shows the electrical conductivity change of AgVO_3 with inverse temperature. In the case of $\alpha\text{-AgVO}_3$ (Fig. 3a), the absolute change of conductivity varies

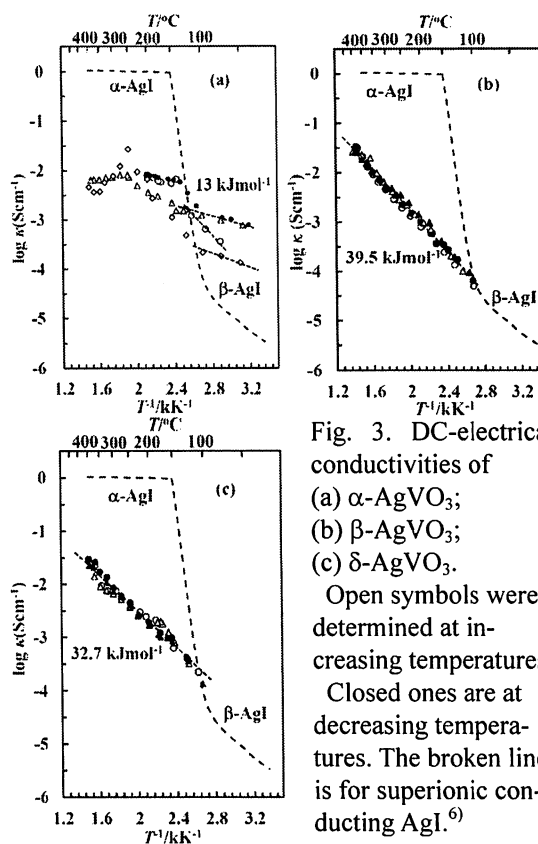


Fig. 3. DC-electrical conductivities of (a) $\alpha\text{-AgVO}_3$; (b) $\beta\text{-AgVO}_3$; (c) $\delta\text{-AgVO}_3$.

Open symbols were determined at increasing temperatures. Closed ones are at decreasing temperatures. The broken line is for superionic conducting AgI.⁶⁾

from sample to sample. However, repeated measurements gave a rather general understanding that the conductivity increases smoothly with temperature up to around $120 \text{ }^\circ\text{C}$ with an endothermic DSC peak at $144 \text{ }^\circ\text{C}$ in Fig. 4a. This does not coincide with the unchanged structural behavior shown in Fig. 5a and suggests the occurrence of small ionic rearrangements.

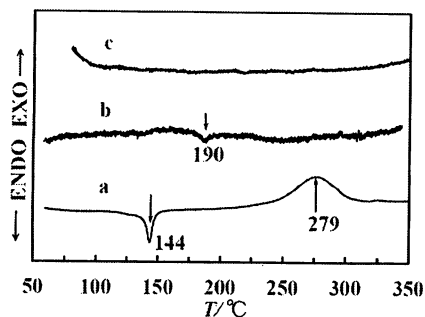


Fig. 4. DSC patterns of α -AgVO₃, β -AgVO₃, and δ -AgVO₃ determined in air at a heating rate of 5 °C min⁻¹.

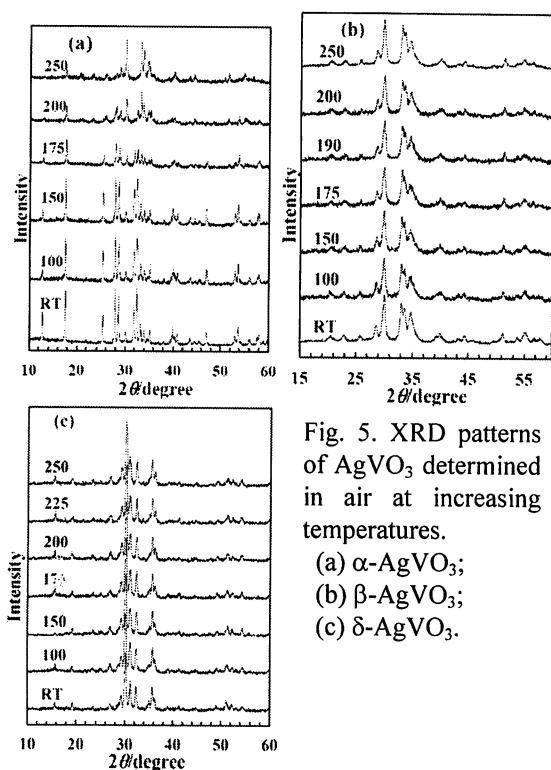


Fig. 5. XRD patterns of AgVO₃ determined in air at increasing temperatures.

(a) α -AgVO₃;
(b) β -AgVO₃;
(c) δ -AgVO₃.

When the α -AgVO₃ was transformed irreversibly into β -AgVO₃ at around 200 °C, the conductivity became less defined, probably because of the break in electrical homogeneity of the solid: fracturing or uncontrolled crystallization of the β -AgVO₃ form.

In the β -AgVO₃ sample shown in Fig. 3b, the plot of electrical conductivity changes linearly with inverse temperature and is reversible. No structural change was detected using powder XRD measurements (Fig. 5b). However, a very tiny endothermic peak was detected at 190 °C on the DSC curve (Fig. 4b). It is anticipated that the thermodynamic change is too small to reflect the electrical and crystallographic changes.

The linear conductivity–inverse temperature relation for δ -AgVO₃ is similar to the β -AgVO₃ phase (Fig. 3c). There is no structural change in the same temperature range (Fig. 5c). There is no signal suggesting a phase change on the DSC curve either (Fig. 4c). Thus, δ -AgVO₃ is a stable phase in this temperature range.

In Figs. 3a–3c, the activation energy values for ionic conductance were determined on the linear part of the plots. It is noted that the activation energy values increase in the order α -AgVO₃ (13 kJ mol⁻¹), δ -AgVO₃ (32.7 kJ mol⁻¹), β -AgVO₃ (39.5 kJ mol⁻¹). This order corresponds to that of molar volume variation, i.e., inverse of the density, 1/4.81 cm³ g⁻¹, 1/5.01 cm³ g⁻¹, and 1/5.39 cm³ g⁻¹, respectively. This fact is related to the larger free space for the silver ions to migrate in the former AgVO₃. However, the ionic conductivity of AgVO₃ is much smaller than that of the typical superionic conductor AgI,⁶⁾ which is shown in Fig. 3a–3c with a broken line.

Figure 6 shows conclusively the free energy–temperature relations of AgVO₃ that are derived from the above measurements. Here, a phase change of the various starting AgVO₃ samples is seen along the line for each substance. With AgVO₃, structurally the β -form is a stable phase, but thermodynamically there is a high-temperature phase β' -AgVO₃. The metastable phases α -AgVO₃ and δ -AgVO₃ are placed at higher positions.

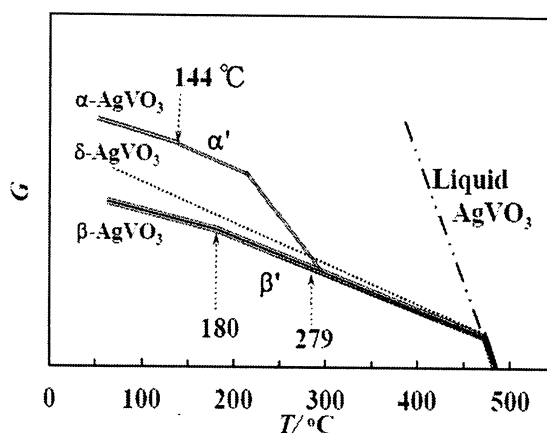


Fig. 6. Imaginary free energy–temperature relations of α -AgVO₃, β -AgVO₃, and δ -AgVO₃. Arrow at 144 °C indicates the reversible transition point of α -AgVO₃; arrow 180 °C, thermodynamic transition point of β -AgVO₃ to β' -type; arrow at 279 °C, the transition from α -AgVO₃ to β -AgVO₃; dotted line is for the δ -AgVO₃.

3. *Crystal structure of δ -AgVO₃*. The crystal structure of δ -AgVO₃ was analyzed in the previous work using powder XRD and electron diffraction, but without a decisive result. Two new techniques were tested for the purpose of crystal analysis. We could obtain some crystalline parameters but have not reached the final structure of the atomic arrangements. Here, some obtained results are presented.

1. Analyses by combining powder XRD and high-intensity single-crystal XRD at SPring-8. Table 1 shows the crystal parameters of δ -AgVO₃ determined using the latter technique. The density of the material, 4.953 g cm⁻³, is very close to the value 5.01

Table 1. Crystal parameter determined by BL02B1 beamline in SPring-8

Crystal System	monoclinic
Space Group	C2 (#5)
Lattice Parameters/Å	
<i>a</i>	18.82(2)
<i>b</i>	3.589(4)
<i>c</i>	17.83(2)
β /deg	112.891(9)
<i>V</i> /Å ³	1109(1)
Z value	4
Density g/cm ³	4.953
<i>R</i> _w	19.5 %

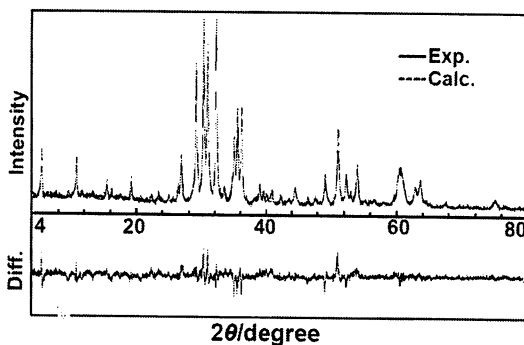


Fig. 7. Rietveld analysis of powder XRD pattern of δ -AgVO₃ with *R*_w = 13.11%.

g cm⁻³ determined using pycnometry. By using the crystal parameters and the atomic arrangements obtained by the single-crystal analysis, Rietveld analysis was conducted on the powder XRD patterns to give the results in Table 2 and the fitted XRD pattern in Fig. 7. However, the obtained atomic arrangements are not chemically acceptable, although the *R*_w value was markedly improved from 19.35 to 13.11.

Table 2 Crystal parameter refined by powder XRD and Rietveld analysis

Lattice Parameters/Å			
<i>a</i>		18.82(2)	
<i>b</i>		3.589(4)	
<i>c</i>		17.83(2)	
β /deg		112.891(9)	
<i>R</i> _w		13.11 %	
Ionic positions			
Ag ⁺ (1)	<i>x</i> =0.7193 <i>y</i> =0.5450 <i>z</i> =0.6988	Ag ⁺ (3)	<i>x</i> =0.4259 <i>y</i> =0.0352 <i>z</i> =0.7595
Ag ⁺ (2)	<i>x</i> =0.3897 <i>y</i> =0.0129 <i>z</i> =0.4745	Ag ⁺ (4)	<i>x</i> =0.6156 <i>y</i> =0.0944 <i>z</i> =0.8103
V ⁵⁺ (1)	<i>x</i> =0.4976 <i>y</i> =0.5362 <i>z</i> =0.6350	V ⁵⁺ (3)	<i>x</i> =0.3347 <i>y</i> =0.5586 <i>z</i> =0.8694
V ⁵⁺ (2)	<i>x</i> =0.8056 <i>y</i> =1.0863 <i>z</i> =0.5852	V ⁵⁺ (4)	<i>x</i> =0.5441 <i>y</i> =-0.5085 <i>z</i> =0.9317
O ²⁻ (1)	<i>x</i> =0.2542 <i>y</i> =0.0729 <i>z</i> =1.0000	O ²⁻ (7)	<i>x</i> =0.5981 <i>y</i> =0.4641 <i>z</i> =0.6376
O ²⁻ (2)	<i>x</i> =0.73367 <i>y</i> =1.01203 <i>z</i> =0.61620	O ²⁻ (8)	<i>x</i> =0.7287 <i>y</i> =0.0420 <i>z</i> =0.8071
O ²⁻ (3)	<i>x</i> =0.8098 <i>y</i> =1.5324 <i>z</i> =0.7983	O ²⁻ (9)	<i>x</i> =0.4671 <i>y</i> =0.4479 <i>z</i> =0.5763
O ²⁻ (4)	<i>x</i> =0.6324 <i>y</i> =0.5652 <i>z</i> =0.8775	O ²⁻ (10)	<i>x</i> =0.3257 <i>y</i> =-0.3798 <i>z</i> =0.8995
O ²⁻ (5)	<i>x</i> =0.5419 <i>y</i> =0.5289 <i>z</i> =0.9357	O ²⁻ (11)	<i>x</i> =0.5414 <i>y</i> =-0.5346 <i>z</i> =0.9336
O ²⁻ (6)	<i>x</i> =0.4989 <i>y</i> =1.6817 <i>z</i> =0.6261		

2. By using the crystal parameters obtained from the above experiments and some additional modifications of atomic arrangements, Rietveld analysis was conducted on the ND pattern obtained using Vega at KEK. The fitting was apparently fine with *R*_w value of 9.81, as shown in Fig. 8; however, the

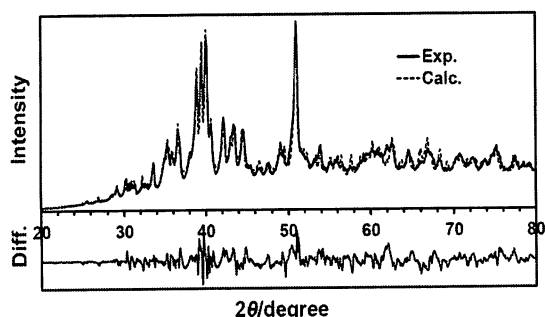


Fig. 8. ND pattern measured using VEGA at KEK, analyzed using Rietveld fitting with $R_w = 9.81\%$.

atomic arrangements do not satisfy the chemical bonding requirements. Therefore, further tests are required before attainment of the final form of the structure.

Conclusions

The ionic conductivities of α -AgVO₃, β -AgVO₃, and δ -AgVO₃ were measured as a function of temperature. β -AgVO₃ and δ -AgVO₃ have superionic conductivities at higher temperatures. The phase transition from α -AgVO₃ to β -AgVO₃ brings about a discontinuous jump in conductivity. β -AgVO₃ showed a slight transition in conductivity despite the absence of a structural change.

The crystal structure of δ -AgVO₃ was analyzed using high-intensity XRD, and neutron-scattering structural parameters were determined; however, the atomic arrangement has not yet been accomplished. Further analysis is expected by preparing a larger crystallite.

Acknowledgments

The authors express sincere thanks to Prof. Kojiro Toriumi for the aide in high-resolution XRD diffraction measurements with BL02B1 beamline in SPring-8.

References

- 1) S. Kittaka, Y. Yata, K. Matsuno, and H. Nishido, *Interaction of Ag ions with a vanadium pentoxide hydrate-Formation of silver vanadate at low temperature*, *J. Mater. Sci.*, **35**, 2185-2192 (2000).
- 2) S. Kittaka, K. Matsuno, and H. Akashi, *Crystal Structure of α -AgVO₃ and Phase Relation of AgVO₃*, *J. Solid State Chem.*, **142**, 360-367 (1999).
- 3) H. Takahashi, K. Shishitsuka, T. Sakuma, Y. Shimojo, and Y. Ishii, *Structure refinement of lithium ion conductors $Li_3Sc_2(PO_4)_3$ and $Li_3-2x(Sc_{1-x}Mx)_2(PO_4)_3$ ($M=Ti, Zr$) with $x=0.10$ by neutron diffraction*, *Solid State Ionics*, **113-115**, 685 (1998).
- 4) J. E. Garbarczyk, M. Wasiucionek, P. Machowski, and W. Jakubowski, *Transition from ionic to electronic conduction in silver-vanadate-phosphate glasses*, *Solid State Ionics*, **119**, 9-14 (1999).
- 5) K. Fueki, *Kagaku no Ryoiki*, **30**, 428 (1975).
- 6) M. R. Johan, T. S. Leng, N. L. Hawari, and S. Suan, *Phase Transition and Complex Impedance Studies of Mechano-Chemically Synthesized AgI-CuI Solid Solutions*, *Int. J. Electrochem. Sci.*, **6**, 6235-6243 (2011).